Heat and Mass Transfer Research Journal
Vol. 2, No. 1; 2018
Published by CanSRG
http://cansrg.com/journals/hmtrj/

A numerical study on enhancement in convective heat transfer from a forcibly oscillating cylinder perpendicular to stream direction

M. Saghafian* and F. Baratchi
Department of Mechanical Engineering, Isfahan University of Technology, Isfahan, 84156, Iran

Abstract

In this paper we use Moving Overset Grids method and study the effect of forced oscillations of a circular cylinder on heat transfer process. In the first part, vibrations of a cylinder with $A/D = 0.25$ and $A/D = 0.4$ are simulated and the effects of driving frequency and lock-in condition on Nusselt number are studied. In the second part, the effects of changes in Reynolds number, amplitude of oscillation and vortex shedding modes, on Nusselt number are investigated.

Keyword: *heat transfer; Nusselt number; forced vibration; lock-in; vortex shedding modes*

1. Introduction

Examples of heat transfer from stationary heated cylinders can be seen in industry commonly. Heated pipes of a heat exchanger, nuclear reactors fuel rods and even hot wire anemometers are some of them. This subject, because of its vast application, has drawn a lot of attentions from scientists. Experimental works of Eckert and Soehngen [1], Churchill and Bernstein [2] and Numerical studies of Jain and Goel [3], Karniadakis [4], Yang et al. [5], Momose and Kimoto [6] and Bharti et al. [7] are some of them.

Despite effects of cylinder oscillation on heat transfer process, much less studies have been conducted on heated vibrating cylinders in a cross flow and most of studies on vibrating cylinder, concern velocity field around the cylinder and imposed forces on it. Between studies on this subject, laboratory work of Sreenivasan and Ramachandran [8] is one of the first which investigated oscillation effect on heat transfer from a circular cylinder in a cross flow. Because of low value of excitation frequency in their work, they did not observe any considerable change in heat transfer coefficient. Leung et al. [9] in their experimental study observed that increase in heat transfer is proportional with oscillation frequency and amplitude. Cheng et al. [10] experimentally studied a range of cylinder oscillation with $0 \leq St_c \leq 0.65$ and $0 \leq A/D \leq 0.628$ (St_c is Strouhal number corresponding to cylinder oscillation frequency, A is oscillation amplitude and D is cylinder diameter) for flows with $0 \leq Re \leq 4000$ and find that lock-in and turbulence are major factors which improve heat transfer. Pottebaum and Gharib [11] in their laboratory work investigated the effects of transverse vibrations of a circular cylinder on its heat transfer process. They examined a wide range of oscillation frequencies and amplitudes and found that heat transfer enhancement is strongly affected by synchronization (lock-in), cylinder wake mode and cylinder transverse velocity.

Due to complicated interaction between fluid and structure, much less numerical work has been conducted in this field. Karanth et al. [12] used a finite difference method and simulated heat transfer from an oscillating cylinder in a flow with $Re = 200$ and investigated in line and transverse oscillation effect on average and distribution of local Nusselt number. Fu and Tong [13] simulated heat transfer from a heated oscillating cylinder using an arbitary Lagrangian-

* Corresponding author
Submitted: February 3, 2018 Accepted: July 5, 2018

Eulerian kinematic description method and examined the effects of Reynolds number, oscillation amplitude and oscillation speed on flow and heat transfer characteristics. Zhang et al. [14] used an immersed boundary method and simulated heat transfer from a stationary and oscillating circular cylinder. They performed this study both for isothermal temperature and iso-heat-flux boundary condition and investigated distribution of local Nusselt number. Nobari and Ghazanfarian [15] used a finite element method based on the Characteristic Based Split method (CBS) to study convective heat transfer from a rotating cylinder with inline oscillation, in a flow with Reynolds numbers of 100, 200 and 300.

In the present work, for the first time, we use Moving Overset Grids method for studying the effect of cylinder oscillation, lock-in phenomenon and vortex shedding modes on heat transfer process. In this method, remeshing step, which in other methods brings many complexities and takes a high value of CPU time, is omitted. So, using this method, simulation of fluid and structure interaction problems, involving an individual or a group of moving objects with different geometries, different types of movements, and different arrangements can be done much easier and faster than other methods. In the next part, a brief description about Moving Overset Grids method is presented.

2. Moving Overset Grids method

The Moving Overset Grids method is a powerful and efficient method with many capabilities for simulating fluid and structure interactions problems. This method uses two types of meshes simultaneously. The first type grid is a major grid which is usually fixed in space, and the second type, is one or a number of minor body fitted grids, constructed around objects, which may be either stationary or moving structures. In the present work, this method is used for simulating the flow field around a transversely oscillating cylinder. The major grid in this study is a rectangular grid, called the static mesh, and the minor grid, called the dynamic grid, is an O-type body fitted grid, constructed around a circular cylinder (located on the rectangular grid). Dynamic and static grids composed together are shown in Figure 1. The flow is solved separately in each grid and the solution variables are transmitted from one grid to the other one by doing interpolation in certain points that are called fringe points.

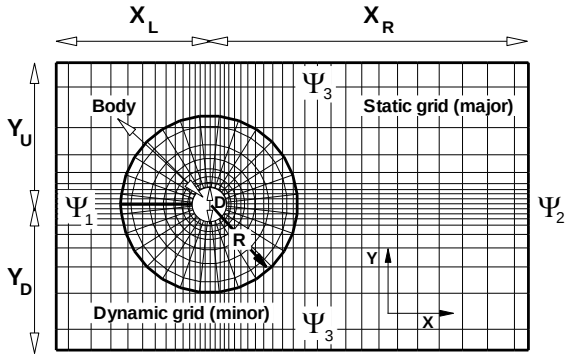

Figure 1. Flow field specifications.

To interpolate the information of a fringe point of either the static or the dynamic grid, surrounding nodes in the other grid should be specified. Hence, an efficient search algorithm is required. The basic concept of this algorithm is adopted from Nirschel et al. [16] and Tuncer [17]. This directional search algorithm localizes the fringe points of each grid in the other one in each time step. Specifying the surrounding nods of each fringe points in other grid, interpolation of information can be done. Several methods are available for interpolating data between two grids. In this work, three different interpolation methods including the Bilinear method, the Inverse Distances method (Wehr et al. [18]), and an interpolation method which

has been derived from the search algorithm (Nirschel et al. [16]; Tuncer [17]) were compared and it was concluded that the last one is the most suitable method which is utilized in this study.

In addition to fringe points, there is another group of special nods which are called hole points. Hole points are those control volumes of the static grid that are located within the cylinder boundary and to which, the dynamic properties of the cylinder are applied. Hole and fringe points are illustrated in Figure 2.

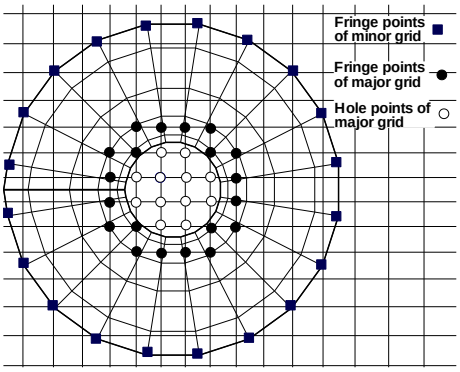

Figure 2. Fringe points and hole points.

3. Governing equations

In this study, the effect of forced oscillations of a circular cylinder in a laminar flow of an incompressible fluid with constant properties is investigated. Because of low viscosity of fluid and its laminar regime, viscous heating effect is neglected. The governing equations are continuity (1), momentum (2) and energy (3) equations as below.

$$\frac{du_i}{dx_i} = 0 \tag{1}$$

$$\frac{du_i}{dt} + u_j \frac{du_i}{dx_j} = \upsilon \frac{d}{dx_j}\left(\frac{du_i}{dx_j}\right) + S \tag{2}$$

$$\frac{dT}{dt} + u_j \frac{dT}{dx_j} = \alpha \frac{d}{dx_j}\left(\frac{dT}{dx_j}\right) \tag{3}$$

In these equations, υ is kinematics coefficient of viscosity and α is the thermal diffusivity of fluid. In equation (2) source term (S) consists of two parts: pressure gradient and effect of accelerating coordinate system. For static grid, second part of source term is zero but for dynamic grid, because of non-inertial coordinate, it should be taken into account. The source terms for the static and the dynamic grids are, therefore, as those in relations (4) and (5), respectively.

$$S = -\frac{dP}{dx_i} \tag{4}$$

$$S = -\frac{dP}{dx_i} - \rho \frac{dV_{c,i}(t)}{dt} = -\frac{dP}{dx_i} - \rho a_{c,i}(t) \tag{5}$$

In these relations, P represents pressure, ρ is density of fluid, $V_{c,i}$ is ith component of cylinder velocity and $a_{c,i}$ is ith component of cylinder acceleration.

4. Boundary conditions

In the static grid, for inlet boundary (Ψ_1, according to Figure 1), we set, $u = U_\infty$, $v = V_\infty = 0$ and $T = T_\infty$. In outlet boundary (Ψ_2), convective boundary condition is used as below.

Table 1. Specifications of static and dynamic grid.

Case	X_L/D	X_R/D	Y_U/D	Y_D/D	R/D	O grid $n_i \times n_j$	O grid $n_i \times n_j$	Δt	Nu Stationary	Nu oscillating
1	15	30	15	15	8	122×92	202×142	0.01	5.056	5.080
2	15	30	15	15	8	142×122	222×162	0.01	5.055	5.074
3	20	40	20	20	10	132×114	262×182	0.01	5.043	5.072
4	15	30	15	15	8	122×92	202×142	0.005	5.058	5.109

$$\frac{du}{dt} + U_\infty \frac{du}{dx} = \frac{dU_\infty}{dt}$$
$$\frac{dv}{dt} + U_\infty \frac{dv}{dx} = 0 \qquad (6)$$
$$\frac{dT}{dt} + U_\infty \frac{dT}{dx} = 0$$

For the distant boundaries (Ψ_3), the gradient of flow variables normal to the boundary are zero. For control volumes of the static grid which are positioned in the vicinity and outside of the body (i.e., the fringe points of the static grid), in each time step, temperature and velocity components are interpolated from the dynamic grid.

In the dynamic grid, no slip condition is applied for the control volumes on the surface of the body and for control volumes on the outer boundary of this grid (fringe points of the dynamic grid), temperature and velocity components are interpolated from the static grid.

In this work, the finite volume approach is applied to discretize differential equations. The SIMPLEC algorithm is employed to solve the discretized equations and the QUICK scheme is used for calculating the convective terms. The Crank-Nicholson time marching method is employed in this work and Rhie-Chow method is used to prevent non-physical oscillations.

5. Grid study

In this numerical approach, as an insurance for appropriate width of flow field, sufficient number of elements in each grid and proper time interval, cases of stationary and vibrating cylinder ($A/D = 0.5$ and $St_c/St_s^* = 0.8$) in a flow with $Re = 100$, are solved for 4 groups of specifications which are presented in Table 1. X_L, X_R, Y_U, Y_D and R notations which are used in this table are shown in Figure 1. St is Strouhal number which is non-dimensional form of frequency and is defined as $t = fD/U\infty$. Strouhal number corresponding to vortex shedding frequency is denoted as $St_s^* = f_sD/U\infty$. Star superscript in St# $*$ represents for stationary cylinder ($St_s^* = f_s^*D/U\infty$) and $St_c^* = f_c^*D/U_\infty$ is the Strouhal number, corresponding to the frequency of cylinder oscillation.

Comparison of the results, given in Table 1, reveals that the specifications in case 1, are good enough and they are used in this work.

6. Results

It is well known that for a stationary cylinder vortex shedding process starts approximately in $Re = 40$. Alternative departure of vortices cause lift, drag and heat transfer coefficients to be periodic. As a starting point, the results of flow and temperature field simulation around a stationary cylinder in a cross flow is presented in this part. In Table 2, St_s^* , $C_{d,av}$ and $C_{l,rms}$ for a stationary cylinder in a flow with $Re = 100$ is presented from different studies. Comparison shows a good agreement between the results of this work with previous studies. Time history of Nusselt number for a stationary cylinder in a flow with $Re = 100$ and $Pr = 0.7$ is shown in

Figure 3. Periodic behavior of this number with small amplitude can be seen in this graph. From this graph, mean value of Nu number for this cylinder is about 5.056.

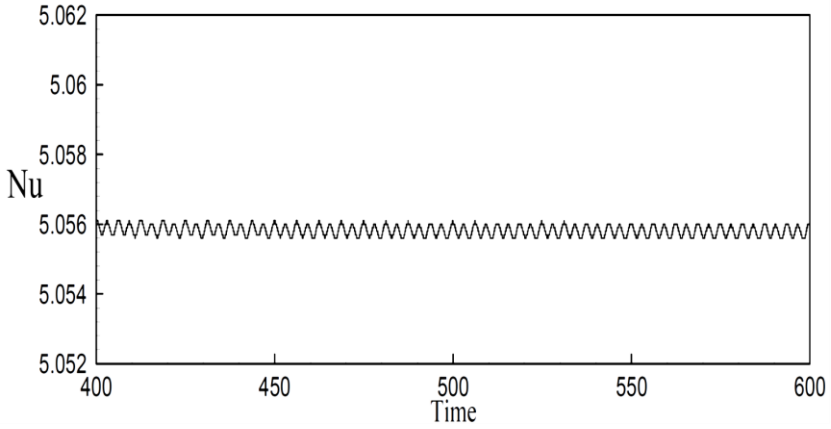

Figure 3. Nusselt number time history for a stationary cylinder; *Re*=100 and *Pr*=0.7.

In Figure 4, average value of Nusselt number of a stationary cylinder versus Re number is shown. One can see that result of present work is in perfect agreement with previous works.

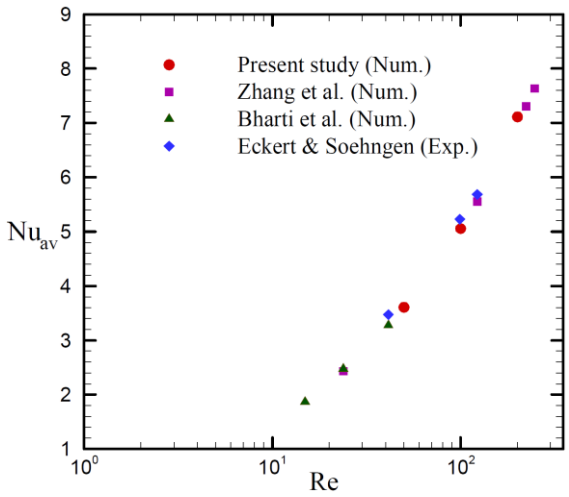

Figure 4. Nu_{av} versus Re for stationary cylinder in a cross flow with *Pr*=0.7.

6.1. Transversely oscillating cylinder

When a cylinder is subjected to vibration, its motion influences the wake and vortex shedding process and dramatically changes aerodynamic and heat transfer characteristics of the cylinder. For transverse oscillation of a circular cylinder with amplitude ratio above a certain threshold ($A/D > 0.05$ according to Koopman) there is a range of frequencies which in this range, vortices departure frequency is equal to excitation frequency, and in other words, vortex shedding is locked to cylinder vibration. In literatures this especial condition is referred as lock-in, synchronization or wake capturing.

In this part; oscillations of a circular cylinder in a flow with $Re = 100$ and $Pr = 0.7$, for two values of vibration amplitude ($A/D = 0.25$ and $A/D = 0.4$) and a wide range of excitation frequencies ($0.4St_s^* - 1.6St_s^*$) are simulated.

For this purpose, position of cylinder is assumed as a sine function of time which is given in relation (7).

$$Y_c(t) = A \sin(2\pi f_c\, t) \tag{7}$$

Once the static grid is constructed over the flow field, knowing the position of cylinder from relation (7), the following steps are taken for simulating the flow in each time step.

1. Construct the dynamic grid;
2. Determine the fringe points of the static and dynamic grids;
3. Localize the fringe points of each grid in the other using search algorithm;
4. Solve the flow field in the static grid using the governing equations and the boundary conditions;
5. Interpolate the temperature and velocity components for the fringe points of the dynamic grid using those of the static grid;
6. Solve the flow field in the dynamic grid using the governing equations and the boundary conditions;
7. Interpolate the temperature and velocity components for the fringe points of the static grid using those of the dynamic grid.

Stages 4 to 7 are repeated until the convergence criterion is satisfied. Estimating temperature and flow variables, lift and drag coefficients and Nusselt number can be calculated. In the next time step, the new position of the cylinder and, thereby, the new position of the dynamic grid is determined and the above procedure is repeated.

Figure 4 shows the (St_c/St_s^*, A/D) plane in which each of investigated cases is shown as a point. Locked cases are shown by solid points and others are represented by hollow ones. Lock-in boundaries achieved by Koopman [19] (*Re*=100):◇, Meneghini and Bearman [20] (*Re*=200): + and Anagnostopoulos [21] (*Re*=106):*****, and results of Nobari and Naderan [22] (*Re*=100):□, Placzek et al. [23] (*Re*=100):∆ and Present work (*Re*=100):○ are shown in this figure.

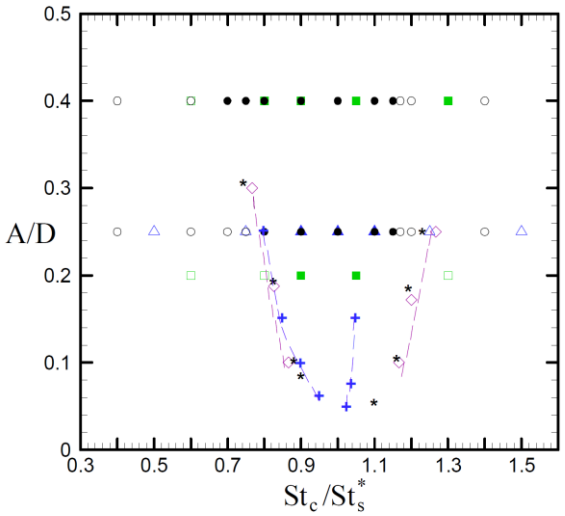

Figure 5. Lock-in region in (St_c/St_s^*, *A/D*) Plane.

Figure 5 indicates that based on results of present work, cases with $St_c/St_s^* = 0.9$ and $St_c/St_s^* = 1.1$, are located within the lock-in range while $St_c/St_s^* = 0.6$ and $St_c/St_s^* = 1.4$ ones are out of the lock-in bounds. Figure 6 shows the changes in the mean value of drag coefficient versus St_c/St_s^* for oscillations with $A/D = 0.25$ and $A/D = 0.4$ in a flow with $Re = 100$ and $Pr = 0.7$. As one can see from these graphs, for low values of excitation frequencies, $C_{d,av}$ (average value of drag coefficient) is approximately equal to the corresponding value for the stationary cylinder (1.341 from Table 2). An increase in the excitation frequency up to the lock-in lower bound makes no significant change in the mean value of the drag coefficient. Within the lock-in range, however, $C_{d,av}$ rises quickly with a large gradient and reaches its maximum value in this range. A similar trend is reported in others work as is illustrated in this figure. As

one can see, there is good agreement between results of present work and previous studies and quantitative differences between the results are due to the differences in simulation conditions and differences in obtained values for the fixed cylinder.

Table 2. St_s^*, $C_{d,av}$ and $C_{l,rms}$ for a stationary cylinder in cross flow with *Re*=100.

STUDY	St_s^*	$C_{d,av}$	$C_{l,rms}$
Tanida et al. (Exp.)	0.14	1.24	
Williamson (Exp.)	0.164	---	
Stansby & Slouti(Num.)	0.166	1.317	0.248
Anagnostopoulos (Num.)	0.167	1.2	
Henderson (Num.)	0.166	1.335	---
Zhou et al. (Num.)	0.162	1.476	0.219
Placzek et al. (Num.)	0.17	1.374	---
Present work (Num.)	0.159	1.341	0.219

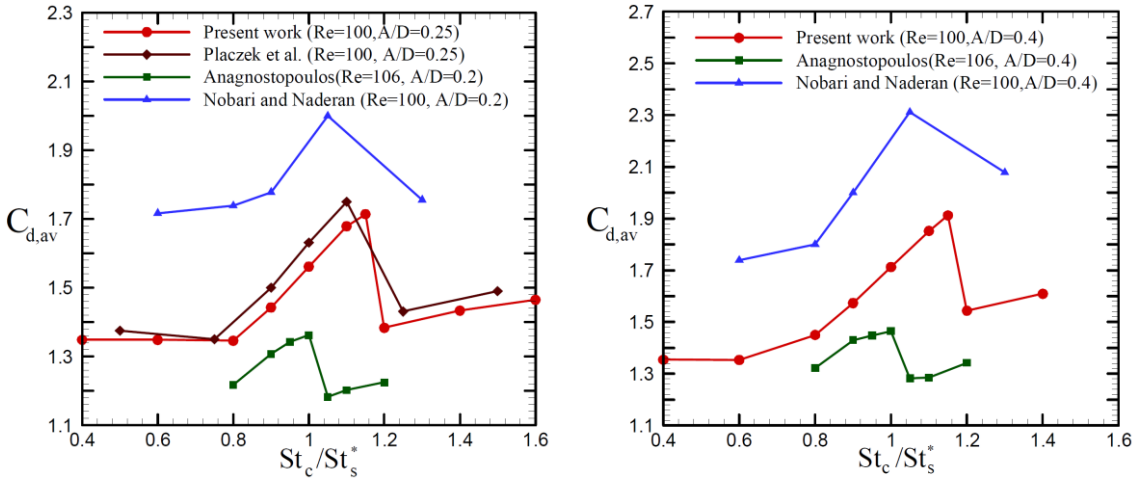

Figure 6. $C_{d,av}$ changes against St_c/St_s^* for oscillations with *A/D*=0.25 and *A/D*=0.4.

In Figure 7, time history of Nusselt number is presented for oscillations with $A/D = 0.25$ and $A/D = 0.4$ in various excitation frequencies in a flow with $Re = 100$ and $Pr = 0.7$.

Comparing this figure with Figure 3 one can see that Nusselt number is dramatically affected with cylinder oscillation. It is obvious that for cases in lock-in region Nusselt number is characterized with constant values for amplitude, frequency and mean value while for unlocked cases a beating pattern can be seen in Nusselt number.

Power spectrum density of Nusselt number for oscillations with $A/D = 0.25$ is shown in Figure 8. It is obvious that for St_c/St_s^* = 0.9 and St_c/St_s^* = 1.1 (cases that are in lock-in region); only one peak can be seen in power spectrum graph which happens in $St = 2St_c$ while for St_c/St_s^* = 0.6 and St_c/St_s^* = 1.4 which are out of lock-in range; two distinctive peaks can be detected: One major and one minor peak. In St_c/St_s^* = 0.6 case, $St = St_s^*/2$ is the major peak (according to Table 2, St_s^* for a flow with $Re = 100$ is 0.159) and $St = 2St_c$ is the minor one but in St_c/St_s^* = 1.4, $St = 2St_c$ is the major and $St = St_s^*/2$ is the minor peak. It means that the effect of vortex shedding frequency from the stationary cylinder disappears in temperature field for locked cases unlike the others.

In Figure 9, changes of Nusselt number versus cylinder position for various excitation frequencies is shown. It is obvious that for St_c/St_s^* = 0.9 and St_c/St_s^* = 1.1 cases which are in lock-in region; there is a unique path that is the result of existence of one frequency in Nusselt

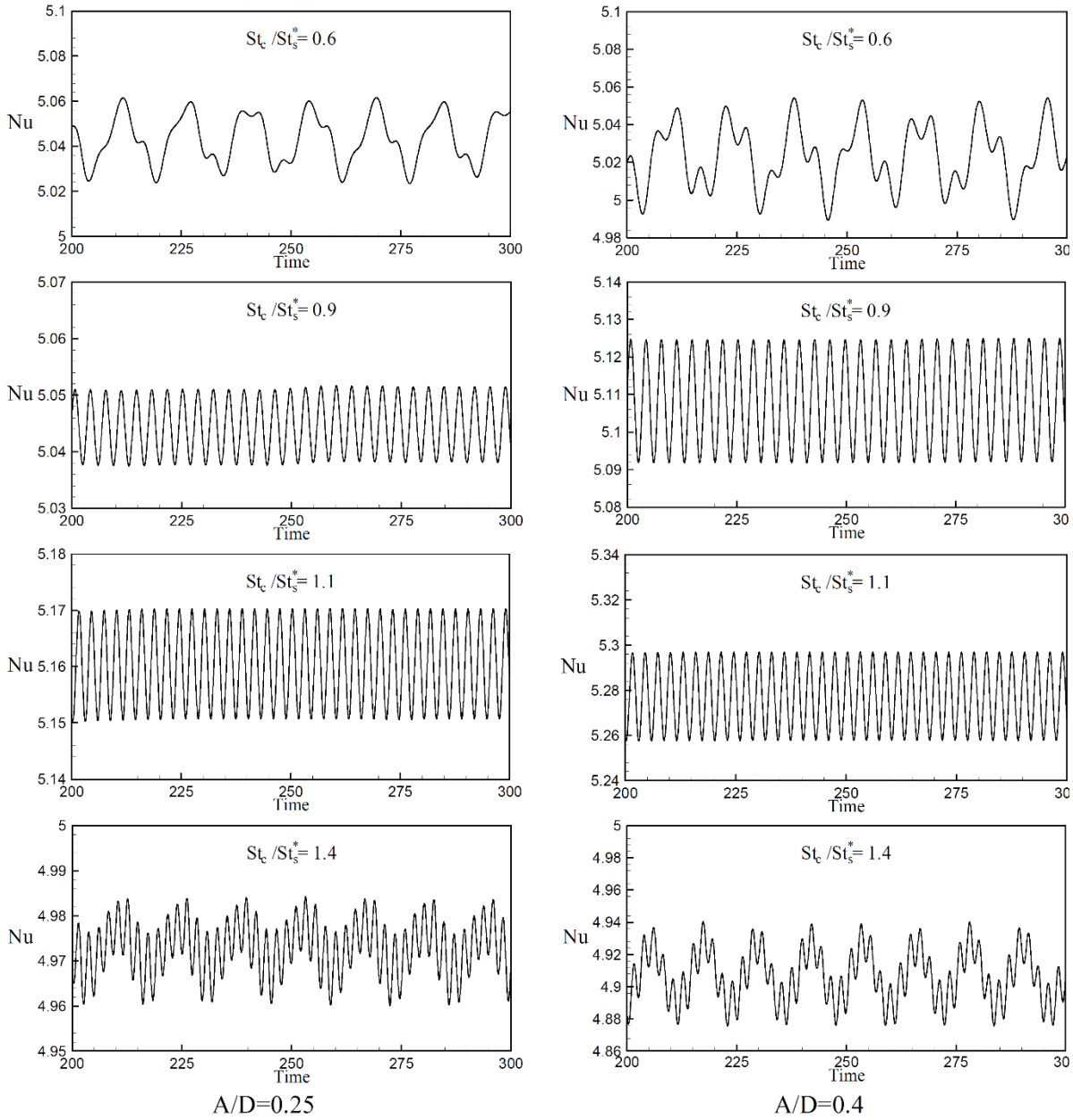

Figure 7. Nusselt number time history; *Re*=100 and *Pr*=0.7.

number but for $St_c/St_s^* = 0.6$ and $St_c/St_s^* = 1.4$; existence of more than one frequency in Nu number, causes many ways in this graph.

It is worth mentioning that synchronization concept can be seen in temperature contours also. For locked cases, formation of temperature contours synchronizes with cylinder motion and temperature contours pattern in the beginning and at the end of a complete cycle, is exactly the same.

In Figure 10 mean value of Nusselt number is plotted for $A/D = 0.25$ and $A/D = 0.4$ versus St_c/St_s^*. It is clear that Nusselt number reaches to its maximum value within lock-in range.

6.2. The effect of amplitude and Reynolds number changes on vortex shedding process and Nusselt number

As is reported in previous works, a variety of vortex shedding patterns can be seen for various combination of excitation frequency and amplitude of oscillation. According to Williamson

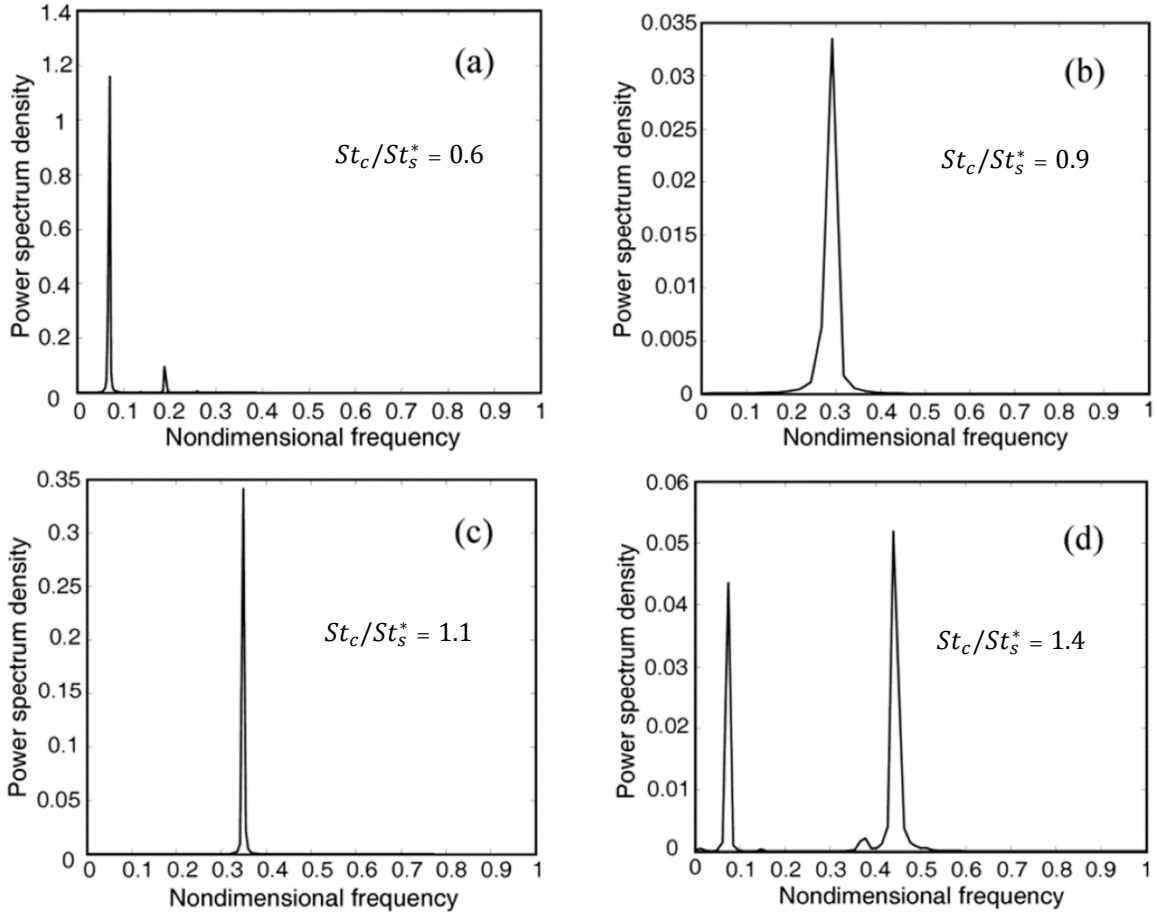

Figure 8. Power spectrum density of Nusselt number; *Re*=100, *A/D*=0.25.

and Roshko [24] for $Re < 300$, 2S and P+S are major vortex shedding patterns near lock-in region.

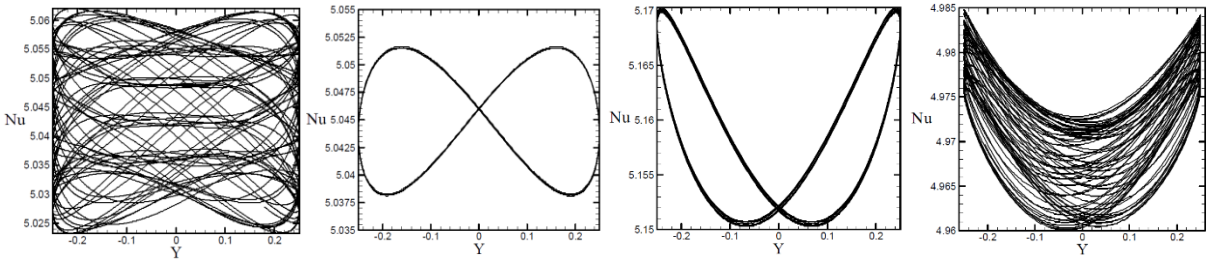

(a) $St_c/St_s^* = 0.6$ (b) $St_c/St_s^* = 0.9$ (c) $St_c/St_s^* = 1.1$ (d) $St_c/St_s^* = 1.4$

Figure 9. Nusselt number against cylinder position; *A/D*=0.25, *Re*=100, *Pr*=0.7.

2S vortex shedding pattern occurred for oscillations with low value of A/D. It means that after a positive vortex which departs in first half cycle of oscillation a negative one is realised in second half cycle of cylinder oscillation. By increasing the vibration amplitude, one can see P+S vortex shedding pattern. In this pattern in a cycle of oscillation a pair of vortices are shed on one side of wake center line and a single vortex on the other side. This form of vortex shedding is reported by Meneghini and Bearman [20], Nobari and Naderan [22] and Placzek et al. [23], also. In Figure 11, vortex shedding pattern for a vibrating cylinder; oscillating with St_c = 0.16 in flows with $Re = 80$ and $Re = 200$ for various amplitude of oscillation up to $A/D = 1$ is depicted. This figure shows that vortex shedding mode remains 2S up to $A/D = 1$ for flow with $Re = 80$. On the other hand, in flow with $Re = 200$, for oscillation with $A/D = 0.7$, vortex shedding mode changes to P+S and remain P+S for $A/D = 1$.

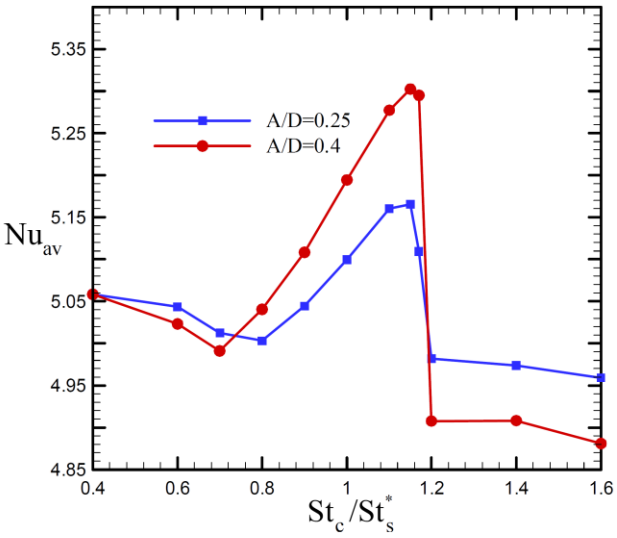

Figure 10. Nu_{av} changes against St_c/St_s^* for *A/D*=0.25 and *A/D*=0.4, *Re*=100, *Pr*=0.7.

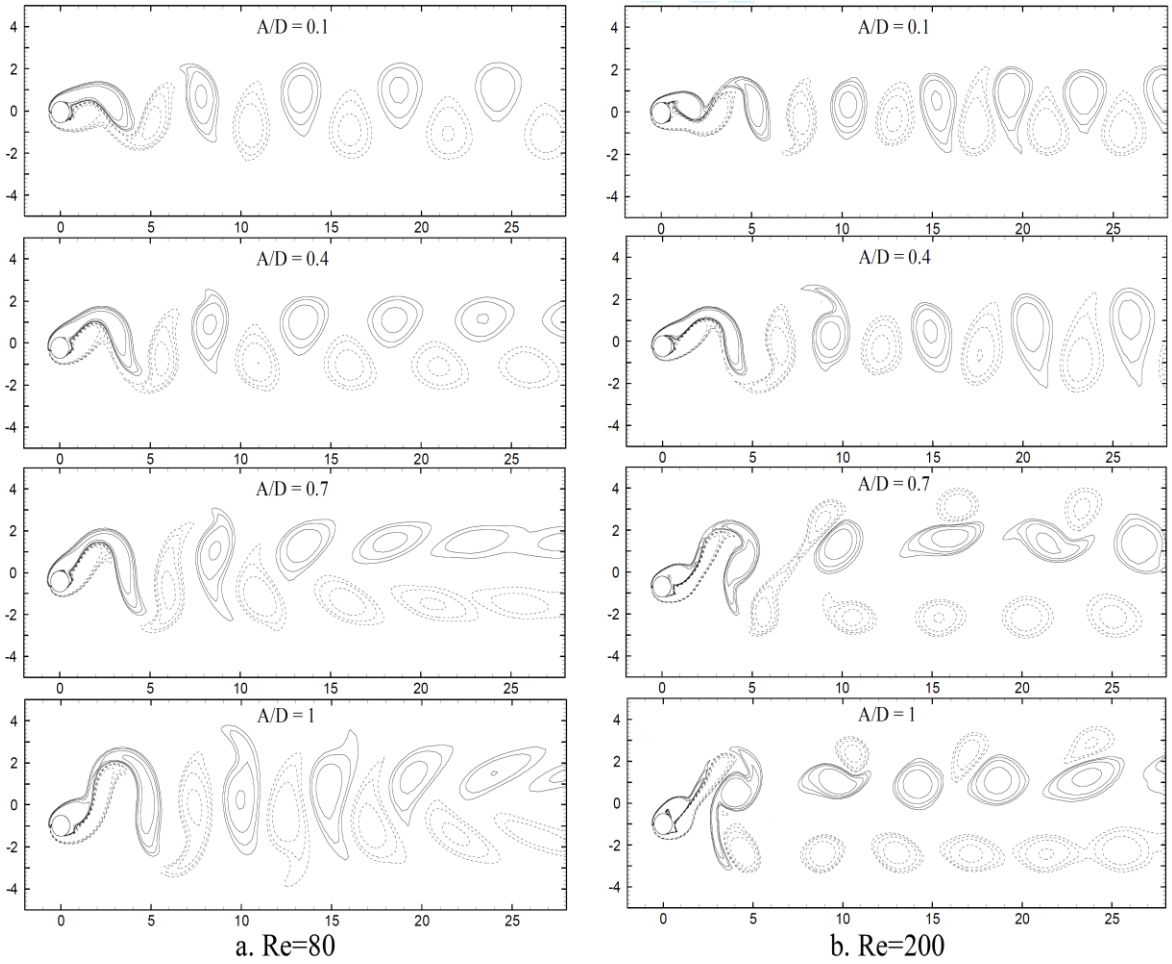

Figure 11. Vortex shedding process from vibrating cylinder with St_c = 0.16, *Pr* = 0.7.

In Figure 12, time history of Nusselt number is given for these cases. As one can see, for $Re = 80$, mean value and amplitude of Nusselt number grows with amplitude of cylinder oscillation continuously. For $Re = 200$, the beating manner in Nu number in $A/D = 0.1$, indicates that

this case is out of the lock-in region. While for $A/D = 0.4$, Nu number is characterized with characteristics of a locked oscillation with 2S vortex shedding mode, $A/D = 0.7$ and $A/D = 1$ cases which are similarly in lock-in zone, show a different pattern in their Nu number time history which happens due to P+S vortex shedding mode. For these two latter cases, there are two distinct peaks in Nu number in each cycle.

In Figure 13, Nu-Y graphs for cases with P+S vortex shedding mode ($A/D = 0.7$ and $A/D = 1$) are shown. As one can see from these graphs, there is only one unique path in their Nu-Y graph, which unlike locked cases with 2S vortex shedding mode, are not symmetric.

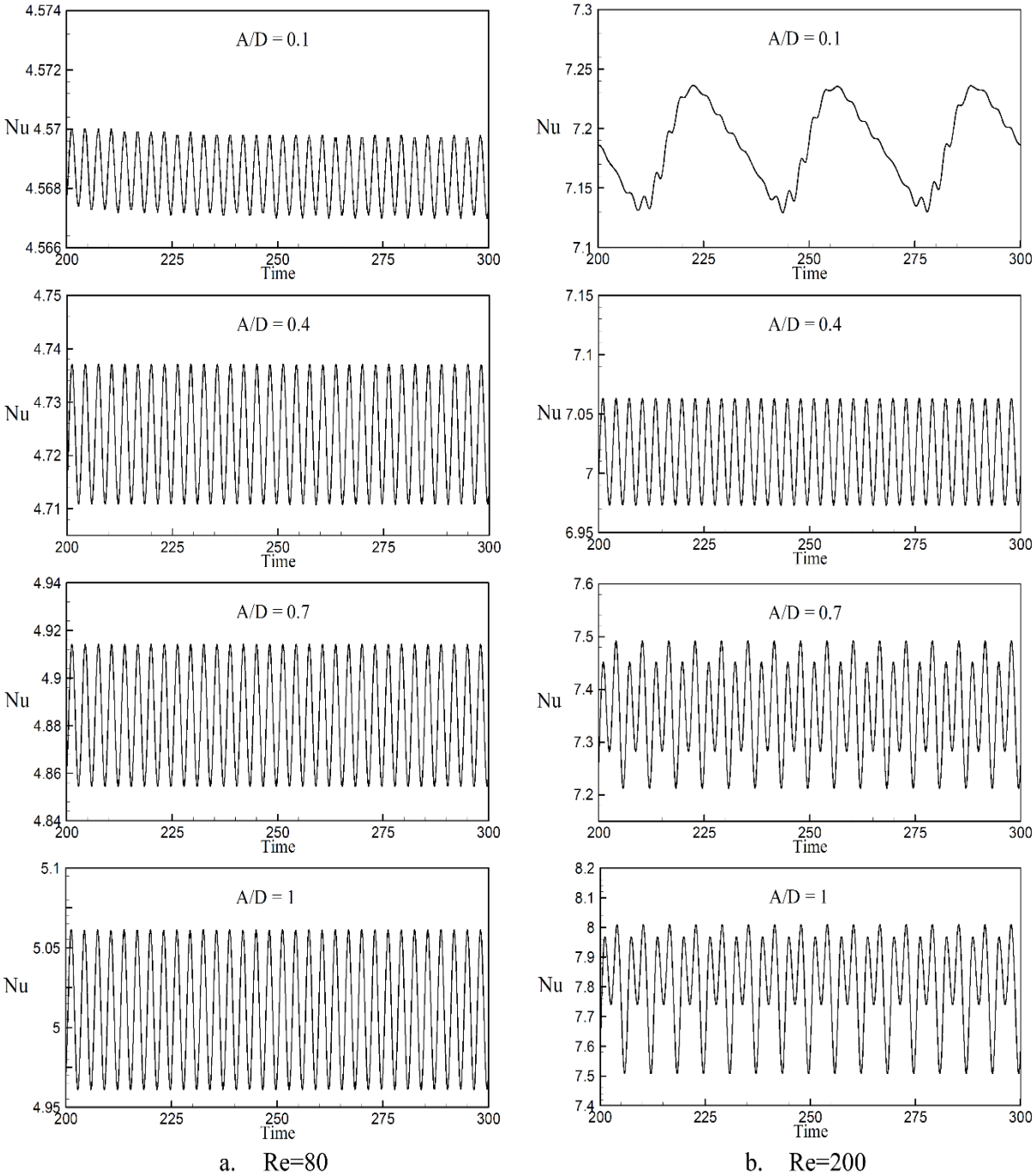

Figure 12. Time history of Nusselt number for vibrating cylinder with $St_c = 0.16$.

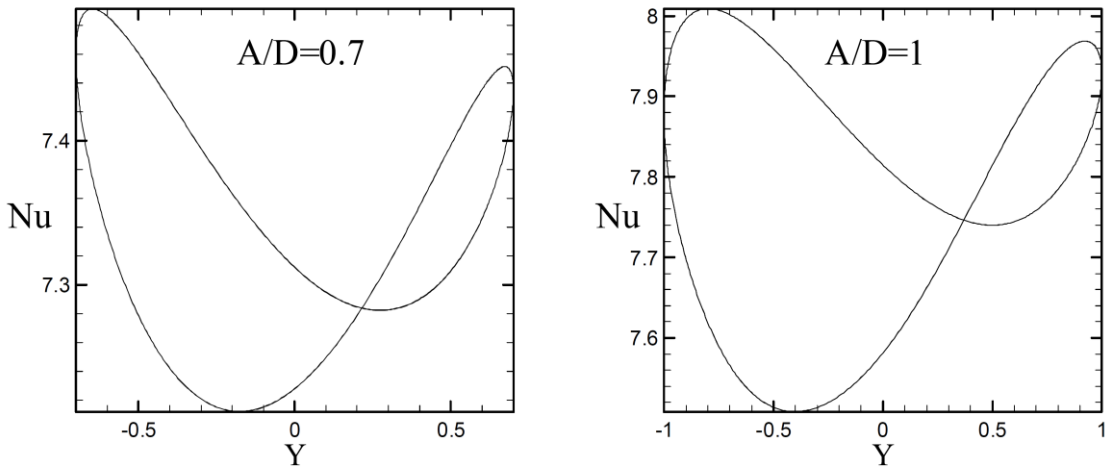

Figure 13. Nusselt number against cylinder position for cases with P+S vortex shedding mode *Re*=200, *Pr* = 0.7.

7. Conclusions

In this work, heat transfer process from a forcibly oscillating cylinder perpendicular to the stream direction in a laminar flow has been simulated using the Moving Overset Grids method. In the first part, flow and temperature fields around a stationary cylinder were preliminarily simulated and Nu number of cylinder in flows with different Re numbers were determined which were in complete agreement with previous works. Then oscillations of a cylinder with $A/D = 0.25$ and $A/D = 0.4$ over a wide range of excitation frequencies around the Strouhal frequency ($0.4St_s^* - 1.6St_s^*$) in a flow with $Re = 100$ and $Pr = 0.7$ was undertaken. In this part, lock-in region was determined, and time history, power spectrum density and Nu-Y graphs
for cases in lock-in region and cases out of lock-in range were presented and characteristics of them were discussed. It can be summarized that, locked cases are characterized with solid time history graph, one pick in power spectrum density graph and one unique path in Nu-Y graph. Then average value of Nusselt number versus excitation frequency was depicted and it was shown that Nu number reaches its maximum value in lock-in range. In the last part of this study, oscillations of a cylinder with St_c = 01.6 were investigated for various values of oscillation amplitudes up to $A/D = 1$ in flows with $Re = 80$ and $Re = 200$ and the effects of *Re* number, vibration amplitude and vortex shedding mode on Nusselt number were investigated.

References

[1] E. Eckert and E. Soehngen, Distribution of heat transfer coefficients around circular cylinder in cross flow at Reynolds numbers from 20 to 500, Transactions of the ASME, vol 74, pp. 343-347, 1952.

[2] S.W. Churchill and M. Bernstein, A correlating equation for forced convection from gases and liquids to a circular cylinder in cross flow, Journal of Heat Transfer, vol 99(2), pp. 300-306, 1977.

[3] P.C. Jain and B.S. Goel, A numerical study of unsteady laminar forced convection from a circular cylinder, Journal of Heat Transfer, vol 98, pp. 303-307, 1976.

[4] G.E. Karniadakis, Numerical simulation of forced convection heat transfer from a cylinder in cross flow, International Journal of Heat and Mass Transfer, vol 31, pp. 107-118, 1988.

[5] Y.T. Yang, C.K. Chen and S. Wu, Transient laminar forced convection from a circular cylinder using a body-fitted coordinate system, Journal of Thermophysics and Heat Transfer, vol 6, pp. 184-188, 1992.

[6] K. Momose and H. Kimoto, Forced convection heat transfer from a heated circular cylinder with arbitrary surface temperature distributions, Heat Transfer-Asian Res. Vol 28(6), pp. 484-499, 1999.

[7] R.P. Bharti, R.P. Chhabra and V. Eswaran, A numerical study of the steady forced convection heat transfer from an unconfined circular cylinder, Heat and Mass Transfer, vol 43, pp. 639-648, 2007.

[8] K. Sreenivasan and A. Ramachandran, Effect of vibration on heat transfer from a horizontal cylinder to a normal air stream, International Journal of Heat and Mass Transfer, vol 3, pp. 60-67, 1961.

[9] C.T. Leung, N.W.M. Ko and K.H. Ma, Heat transfer from a vibrating cylinder, Journal of Sound and Vibration, vol 75(4), pp. 581-582, 1981.

[10] C.H. Cheng, H.N. Chen and W. Aung, Experimental study of the effect of transverse oscillation on convection heat transfer from a circular cylinder, Journal of Heat Transfer, vol 119, pp.474-482, 1997.

[11] T. Pottebaum and M. Gharib, Using oscillations to enhance heat transfer for a circular cylinder, International Journal of Heat and Mass Transfer, vol 49(17-18), pp. 3190-3210, 2006.

[12] D. Karanth, G.W. Rankin and K. Sridhar, A finite difference calculation of forced convective heat transfer from an oscillating cylinder, International Journal of Heat and Mass Transfer, vol 37, pp. 1619–1630, 1994.

[13] W.S. Fu and B.H. Tong, Numerical investigation of heat transfer from a heated oscillating cylinder in a cross flow, International Journal of Heat and Mass Transfer, vol 45, pp. 3033-3043, 2002.

[14] N. Zhang, Z.C. Zheng and S. Eckels, Study of heat-transfer on the surface of a circular cylinder in flow using an immersed-boundary method, International Journal of Heat and Fluid Flow, vol 29(6), pp. 1558-1566, 2008.

[15] M.R.H. Nobari and J. Ghazanfarian, Convective heat transfer from a rotating cylinder with inline oscillation, International Journal of Thermal Sciences, vol 49(10), pp. 2026-2036, 2010.

[16] H. Nirschl, H.A. Dwyer and V. Denk, Three-dimensional calculations of the simple shear flow around a single particle between two moving walls, Journal of Fluid Mechanics, vol 283, pp. 273-285, 1995.

[17] H. Tuncer, Two-dimensional unsteady Navier-Stokes solution method with Moving Overset Grids, AIAA journal, vol 35(3), pp. 471-476, 1997.

[18] D. Wehr, R. Stangl and S. Wagner, Interpolation schemes for intergrid boundary value transfer applied to unsteady transonic flow computations on overlaid embedded grids, Proceeding of the 2th European Computational Fluid Dynamics Conference, Stuttgart, Germany, vol 1, pp. 382-390, 1994.

[19] G.H. Koopman, The vortex wakes of vibrating cylinders at low Reynolds numbers, Journal of Fluid Mechanics, vol 28, pp. 501-512, 1967.

[20] J.R. Meneghini and P.W. Bearman, Numerical simulation of high amplitude oscillatory flow about a circular cylinder, Journal of Fluids and Structures, vol 9, pp. 435-455, 1995.

[21] P. Anagnostopoulos, Numerical study of the flow past a cylinder excited transversely to the incident stream. Part1: Lock-in zone, hydrodynamic forces and wake geometry, Journal of Fluids and Structures, vol 14, pp. 819-851, 2000.

[22] M.R.H. Nobari and H. Naderan, A numerical study of flow past a cylinder with cross flow and inline oscillation, Computers & Fluids, vol 35, pp. 393-415, 2006.

[23] A. Placzek, J. Sigrist and A. Hamdouni, Numerical simulation of an oscillating cylinder in a cross-flow at low Reynolds number: Forced and free oscillations, Computers & Fluids, vol 38, pp. 80-100, 2009.

[24] C.H.K. Williamson and A. Roshko, Vortex formation in the wake of an oscillating cylinder. Journal of Fluid and Structures, vol 2, pp. 355-381, 1988.